



Modelling and Testing the Dynamic Properties of a Launcher with Unguided Missiles

Zbigniew J. DZIOPA^{1*}, Maciej NYCKOWSKI²

¹Kielce University of Technology,
7 Tysiąclecia Państwa Polskiego Ave., 25-314 Kielce, Poland

²Lukasiewicz Research Network – Institute of Aviation
110/114 Krakowska Ave., 02-256 Warsaw, Poland

*Corresponding author's e-mail address and ORCID:
zdziopa@tu.kielce.pl; <https://orcid.org/0000-0002-9135-6306>

*Received: July 15, 2022 / Revised: September 20, 2022 / Accepted: December 12, 2022/
Published: December 30, 2022.*

DOI 10.5604/01.3001.0016.1457

Abstract. The work analyses the operation of the ZSMU-70 weapon module. The results allowed for the development of several guidelines, aiming to shape the dynamic properties of the WW-4 launcher in order to improve the effectiveness of the ZSMU-70 module. This meant that research was carried out at a military training ground. Unguided NLPR-70 missiles were launched. The launching process was recorded using a Phantom high-speed digital camera. The recorded images were then analysed using TEMA software. Based on the results of empirical research, a physical and mathematical model of the motion was formulated for both the ZSMU-70 module as well as the WW-4 launcher. A computer programme was developed, and the motion of the system was simulated during the launching of the missiles.

The results of the theoretical analysis were compared with the analogous results from the empirical research. Having the theoretical model verified, some system parameters were changed, and guidelines were used to improve the effectiveness of the ZSMU-70 weapon module.

Keywords: mechanical engineering, launcher, missiles, empirical research, theoretical analysis

1. INTRODUCTION

The object of research is the ZSMU-70 Remote Controlled Weapon Module, presented in Fig. 1. This module consisted of a TUR-2 armoured vehicle (manufactured by AMZ Kutno, Poland), on which the WW-4 launcher with a system of four tubular guides was mounted. In each of the guides there was an unguided NLPR-70 missile. These missiles were produced by MESKO SA in Skarżysko-Kamienna (Poland) under license and with the use of components produced by Nammo (Nordic Ammunition Company – Norway).



Fig. 1. ZSMU-70 weapon module

The main goal of the work is to develop guidelines aimed at shaping the dynamic properties of the launcher in such a way that the ZSMU-70 weapon module hits the target. In order to complete the work:

- An analysis of images was carried out, recorded using a Phantom v.9.1 high-speed digital camera on the military training ground in Nowa Dęba (Poland). The movement of unguided NLPR-70 missiles, WW-4 launcher with separation of platform and guides, and TUR-2 armoured vehicle was recorded. The TEMA in use program, under which training was conducted by the EC Training Centre, allowed:
 - Determination of the time variation of kinematic quantities describing the movement of individual assembly objects.

- Assessment of the impact of rocket engine activation, missile movement in the guide and the change resulting from the missile leaving the launcher on the behaviour of the assembly.
- Determination of the initial flight parameters of each unguided missile launched.
- Assessing the impact of the gases emitted by the rocket engine on the launcher.
- Determination of the trajectory of the first flight phase of each of the launched missiles.
- The physical and mathematical model of the ZSMU-70 weapon module movement was formulated, in which the conditions of virtual space behave like a real object:
 - The article presents three models of the ZSMU-70 weapon module.
 - The basic dynamic characteristics of the system were determined.
 - The curves of time variation of kinematic quantities describing the movement of individual objects of the assembly model were compared with the real system.
 - A model of the first phase of the unguided missile flight was developed and the obtained results were compared with the trajectory factors obtained from the tests at the military training ground.
 - Guidelines have been developed in order to shape the dynamic characteristics of the system in such a way that the missiles fired in sequence hit the designated target, beginning at shorter time intervals. The dynamic characteristic of the system was understood as a set of physical parameters defining the system and influencing the form of the modal matrix and the responses of the system subjected to excitations.

2. EXPERIMENTAL TESTS

The testing was carried out at the military training ground in Nowa Dęba (Poland). While a missile was leaving the launcher, the effects of the exhaust gases made it difficult to follow the reference point, partially covering the front part of the guide. The correlation option was used to track the points of the guide, which by adjusting the shades of the pixels of an image fragment allowed the tracking of a selected point. The use of image filters, increasing the contrast of the examined point and making it easier to track, was helpful in analysing the results. Difficulties resulting from the registration of the movement of some points introduced an error which, after averaging the obtained results, was estimated at about 10%.

More than twenty NLPR-70 missile launches have been registered (Fig. 2) from the WW-4 launcher (Fig. 3) placed on a TUR-2 armoured vehicle (Fig. 4) [1, 2]. Recorded videos were analysed with the Phantom v.9.1 high-speed digital camera using the specialized TEMA program.

This provided reliable curves of the variability of kinematic quantities as a function of time characterizing the movement of the above-mentioned individual objects of the ZSMU-70 module.



Fig. 2. Unguided NLPR-70 missile



Fig. 3. WW-4 launcher



Fig. 4. TUR-2 armoured vehicle

The article presents a representative example of the angular displacement of the launcher in tilt motion, its angular velocity and angular acceleration, see Fig. 5, Fig. 6 and Fig. 7. The characteristics of the kinematic quantities presented in the example were to be considered as a reference.

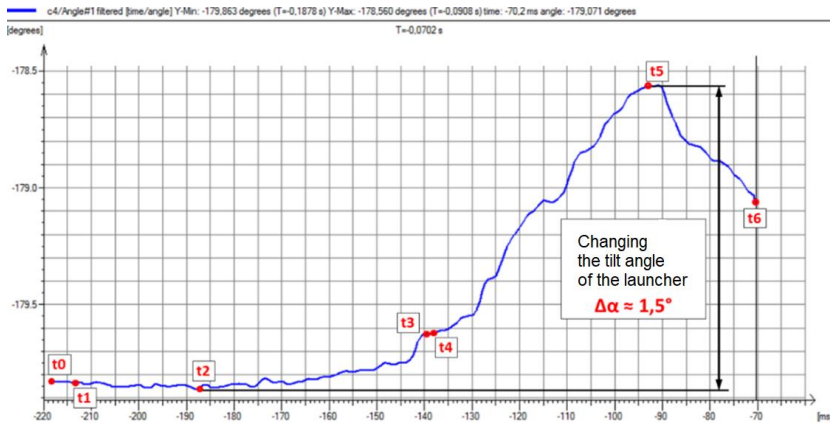


Fig. 5. Angular displacement of the launcher in tilt motion

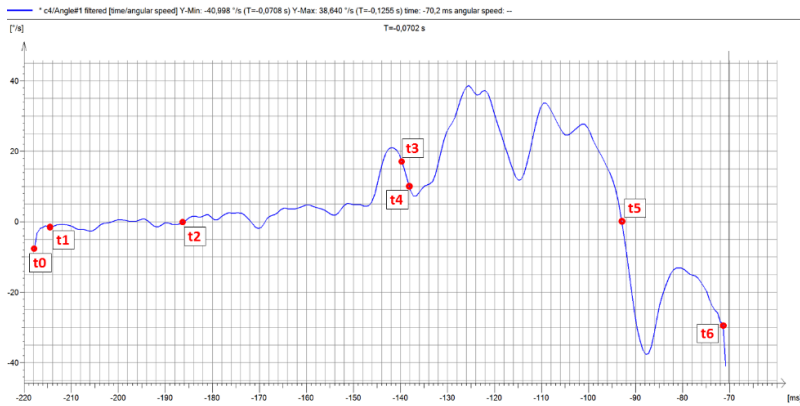


Fig. 6. Angular velocity of the launcher in tilt motion

The graphs refer to the launch of a single missile. The item [3] in the literature list was a reference to the launch dynamics of the missile from the launcher. The characteristic moments of time were plotted on the graphs:

$t_0 = 0$ [ms] – start of recording the unguided missile launch;

$t_1 = 5.295$ [ms] – rocket engine start;

$t_2 = 33.5$ [ms] – missile motion inside the guide;

$t_3 = 80.556$ [ms] – missile moved to the guide end;

$t_4 = 81.144$ [ms] – unguided missile leaves the launcher;

$t_5 = 125.144$ [ms] – the maximum impact of the exhaust gases on the launcher;

$t_6 = 148.764$ [ms] – missile moving away from the launcher with the decreasing impact of exhaust gases emitted by the rocket engine

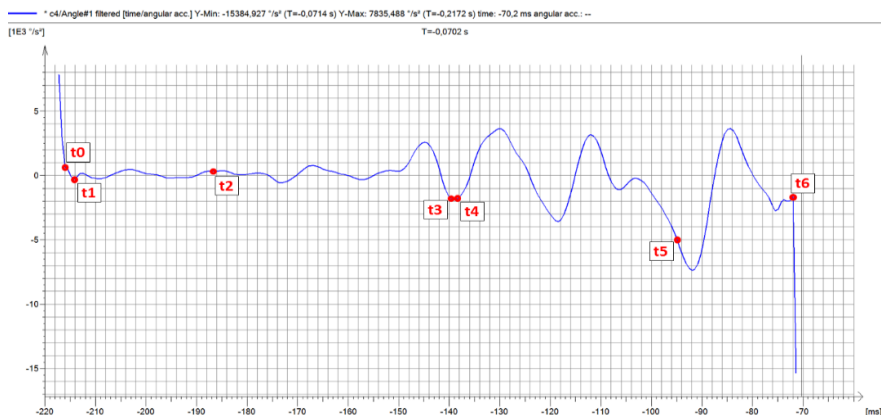


Fig. 7. Angular acceleration of the launcher in tilt motion

The negative time appearing on the graphs results from the specificity of process registration and their interpretation by the TEMA program. The time values read from the graphs should be subtracted from the initial time, t_0 .

3. THEORETICAL ANALYSIS

3.1. Model 1 – ZSMU-70 weapon module

At the beginning of the theoretical analysis, the physical model 1 of the ZSMU-70 weapon module was formulated, Fig. 8 [4]. The body with the launcher makes a perfectly rigid body with a mass equal to m and moment of inertia equal to I . The radial susceptibility characteristics of the front and rear tires together with the susceptibility characteristics of the front and rear suspension were linear Voigt-Kelvin models.

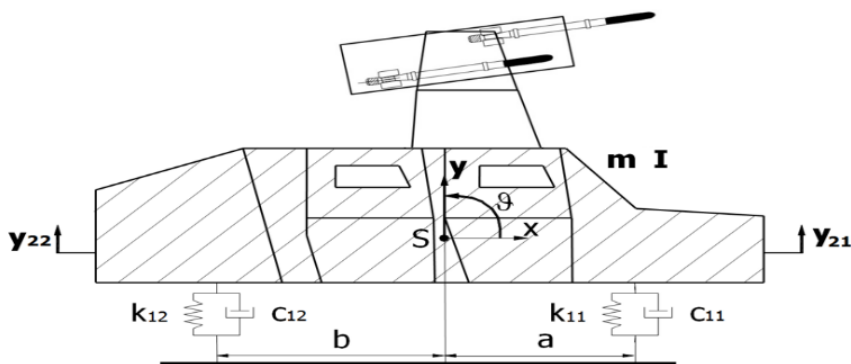


Fig. 8. Physical model 1 of the ZSMU-70 weapon module

Accordingly, the characteristics of weightless deformable elements were represented by the following stiffness and damping coefficients: k_{11} and c_{11} or k_{12} and c_{12} . The a and b dimensions represent the position of the weightless elements in relation to the mass centre of the system. Quantities y and ϑ were independent coordinates that determine the movement of the system.

Using the energy method, a mathematical model of the ZSMU-70 weapon module was derived in the form of a non-storage and autonomous system [5] [6]:

$$\begin{aligned} m\ddot{y} + (c_{11} + c_{12})\dot{y} + (c_{11}a - c_{12}b)\dot{\vartheta} + (k_{11} + k_{12})y + (k_{11}a - k_{12}b)\vartheta = 0 \\ I\ddot{\vartheta} + (c_{11}a^2 + c_{12}b^2)\dot{\vartheta} + (c_{11}a - c_{12}b)\dot{y} + (k_{11}a^2 + k_{12}b^2)\vartheta \\ + (k_{11}a - k_{12}b)y = 0 \end{aligned} \quad (1)$$

System parameter values:

$$\begin{aligned} m = 1780 \text{ [kg]} & \quad I = 2620 \text{ [kgm}^2\text{]} \\ k_{11} = 75000 \left[\frac{N}{m} \right] & \quad k_{12} = 65000 \left[\frac{N}{m} \right] \\ c_{11} = 2000 \left[\frac{Ns}{m} \right] & \quad c_{12} = 2000 \left[\frac{Ns}{m} \right] \\ a = 1.14 \text{ [m]} & \quad b = 1.28 \text{ [m]} \end{aligned}$$

Frequencies and free vibration forms were then determined [7]. After solving the generalised own problem, the secular equation was derived from the characteristic determinant:

$$\begin{aligned} mIs^4 + (mc_{2\vartheta} + Ik_{1y})s^3 + (mk_{2\vartheta} + Ik_{1y} + c_{1y}c_{2\vartheta} - c_{2y}c_{1\vartheta})s^2 + \\ (c_{1y}k_{2\vartheta} + k_{1y}c_{2\vartheta} - c_{2y}k_{1\vartheta} - k_{2y}c_{1\vartheta})s + k_{1y}k_{2\vartheta} - k_{1\vartheta}k_{2y} = 0 \end{aligned}$$

where:

$$\begin{aligned} k_{1y} = k_{11} + k_{12} & \quad k_{1\vartheta} = k_{11}a - k_{12}b \\ k_{2y} = k_{11}a - k_{12}b & \quad k_{2\vartheta} = k_{11}a^2 + k_{12}b^2 \\ c_{1y} = c_{11} + c_{12} & \quad c_{1\vartheta} = c_{11}a - c_{12}b \\ c_{2y} = c_{11}a - c_{12}b & \quad c_{2\vartheta} = c_{11}a^2 + c_{12}b^2 \end{aligned}$$

The obtained elements of the secular equation were imaginary and coupled in pairs:

$$\begin{aligned} s_1 = -h_1 + i\omega_{*1} & \quad s_2 = -h_1 - i\omega_{*1} \\ s_3 = -h_2 + i\omega_{*2} & \quad s_4 = -h_2 - i\omega_{*2} \end{aligned}$$

where:

$$h_1 = 1.185284 \quad h_2 = 1.0596856$$

Free vibration frequencies of the system:

$$\omega_{*1} = 8.7030776 \frac{\text{rad}}{\text{s}} \quad \omega_{*2} = 8.8447087 \frac{\text{rad}}{\text{s}}$$

Free vibration forms:

- First form of free vibrations

$$\omega_{*1} = 8.7030776 \frac{\text{rad}}{\text{s}}$$

$$\mu_{*21} = \mu_{21} e^{i\varphi_1} \quad \mu_{*22} = \mu_{21} e^{-i\varphi_1}$$

$$\varphi_1 = 0.1698824$$

hence

$$\mu_{11} = 1 \quad \mu_{21} = -0.9767338$$

- Second form of free vibrations

$$\omega_{*2} = 8.8447087 \frac{\text{rad}}{\text{s}}$$

$$\mu_{*23} = \mu_{22} e^{i\varphi_2} \quad \mu_{*24} = \mu_{22} e^{-i\varphi_2}$$

$$\varphi_2 = -0.1725998$$

hence

$$\mu_{12} = 1 \quad \mu_{22} = 0.6973517$$

As a result of the considerations, the equations describing free vibrations were obtained in the form:

$$y = A_{11} e^{-h_1 t} \cos(\omega_{*1} t + \alpha_1) + A_{12} e^{-h_2 t} \cos(\omega_{*2} t + \alpha_2)$$

$$\vartheta = \mu_{21} A_{11} e^{-h_1 t} \cos(\omega_{*1} t + \alpha_1 + \varphi_1) + \mu_{22} A_{12} e^{-h_2 t} \cos(\omega_{*2} t + \alpha_2 + \varphi_2)$$

An example of the variability curve of independent coordinates is shown in Fig. 9. Due to the nature of the analysis, the functions obtained cannot be compared with the results obtained in a real shooting. Such a comparison is presented in Fig. 14.

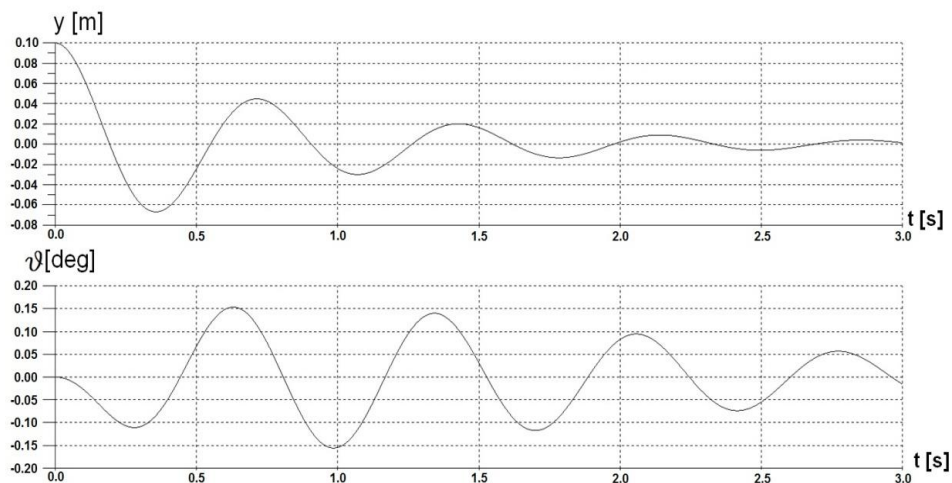


Fig. 9. Variability curve of independent coordinates of the system

3.2. Model 2 and 3 – WW-4 launcher

Model 2

To determine the kinematic quantities characterizing the motion of the launcher-missile system, a physical and mathematical model 2 with five degrees of freedom was formulated, Fig. 11, equations 2 and 3. The obtained results were compared with those obtained from the experimental tests, Fig. 14. The actual launcher-missile system is shown in Fig. 10. After obtaining a satisfactory accuracy, the selected parameters characterizing the launcher were verified, Fig. 15.



Fig. 10. Actual missile-launcher system

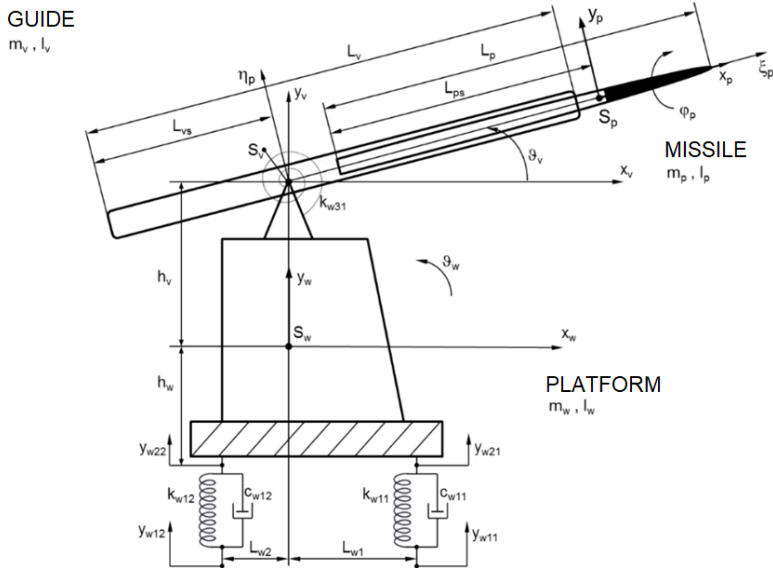


Fig. 11. Physical model 2 of the launcher-missile system

Motion equations (2) of the missile-launcher system:

Platform

$$\begin{aligned}
& (m_w + m_v + m_p)\ddot{Y}_w - (m_v + m_p)h_v\ddot{\vartheta}_w\sin\vartheta_w + m_p\xi_p\ddot{\vartheta}_v\cos\vartheta_v \\
& - (m_v + m_p)h_v\dot{\vartheta}_w^2\cos\vartheta_w - m_p\xi_p\dot{\vartheta}_v^2\sin\vartheta_v + m_p\xi_p\dot{\vartheta}_v\cos\vartheta_v \\
& + k_{w11}\lambda_{w11} + k_{w12}\lambda_{w12} + c_{w11}\dot{\lambda}_{w11} + c_{w12}\dot{\lambda}_{w12} = -(m_w + m_v + m_p)g \\
& \quad \left[I_w + I_{p_{z_p}} + I_v + (m_v + m_p)h_v^2 \right] \ddot{\vartheta}_w \\
& \quad + \left[I_{p_{z_p}} m_p h_v \xi_p (\cos\vartheta_w \sin\vartheta_v - \sin\vartheta_w \cos\vartheta_v) \right] \ddot{\vartheta}_v \\
& - (m_v + m_p)h_v\ddot{Y}_w\sin\vartheta_w - m_p h_v \ddot{\xi}_p (\cos\vartheta_w \cos\vartheta_v + \sin\vartheta_w \sin\vartheta_v) \\
& \quad + 2m_p h_v \dot{\xi}_p \dot{\vartheta}_w \sin\vartheta_w \cos\vartheta_v - 2m_p h_v \dot{\xi}_p \dot{\vartheta}_v \sin\vartheta_w \cos\vartheta_v \\
& \quad + m_p h_v \xi_p \dot{\vartheta}_v^2 (\cos\vartheta_w \cos\vartheta_v - \sin\vartheta_w \sin\vartheta_v) \\
& \quad + k_{w11}l_{w1}\lambda_{w11} - k_{w12}l_{w2}\lambda_{w12} - k_{w31}\lambda_{w31} \\
& + c_{w11}l_{w1}\dot{\lambda}_{w11} - c_{w12}l_{w2}\dot{\lambda}_{w12} - c_{w31}\dot{\lambda}_{w31} = (m_v + m_p)gh_v \sin(\vartheta_w + \vartheta_{wst})
\end{aligned}$$

where:

$$\begin{aligned}
\lambda_{w11} &= Y_w + Y_{wst} + l_{w1}(\vartheta_w + \vartheta_{wst}) - Y_{w11} \\
\lambda_{w12} &= Y_w + Y_{wst} - l_{w2}(\vartheta_w + \vartheta_{wst}) - Y_{w12} \\
\lambda_{w31} &= \vartheta_v + \vartheta_{vst} - \vartheta_w + \vartheta_{wst} \\
\dot{\lambda}_{w11} &= \dot{Y}_w + l_{w1}\dot{\vartheta}_w - \dot{Y}_{w11} \\
\dot{\lambda}_{w12} &= \dot{Y}_w - l_{w2}\dot{\vartheta}_w - \dot{Y}_{w12} \\
\dot{\lambda}_{w31} &= \dot{\vartheta}_v - \dot{\vartheta}_w
\end{aligned}$$

Guide

$$\begin{aligned}
& (I_v + I_{p_{z_p}} + m_p\xi_p^2)\ddot{\vartheta}_v + m_p\xi_p\ddot{Y}_w\cos\vartheta_v + \\
& \left[I_{p_{z_p}} + I_v + m_p h_v \xi_p (\cos\vartheta_w \sin\vartheta_v - \sin\vartheta_w \cos\vartheta_v) \right] \ddot{\vartheta}_w \\
& + 2m_p h_v \dot{\xi}_p \dot{\vartheta}_v + m_p h_v \xi_p \dot{\vartheta}_w^2 (\sin\vartheta_w \sin\vartheta_v + \cos\vartheta_w \cos\vartheta_v) \\
& + k_{w31}\lambda_{w31} + c_{w31}\dot{\lambda}_{w31} = -m_p g \xi_p \cos(\vartheta_v + \vartheta_{vst})
\end{aligned}$$

Missile

$$\begin{aligned}
& m_p \ddot{\xi}_p - m_p h_v \ddot{\vartheta}_w (\cos\vartheta_w \cos\vartheta_v + \sin\vartheta_w \sin\vartheta_v) \\
& + m_p \ddot{Y}_w \sin\vartheta_w + m_p h_v \dot{\vartheta}_w^2 (\sin\vartheta_w \cos\vartheta_v - \cos\vartheta_w \sin\vartheta_v) \\
& + m_p \xi_p \dot{\vartheta}_v^2 = -m_p g \sin(\vartheta_v + \vartheta_{vst}) + P_p
\end{aligned}$$

$$I_{p_{x_p}} \ddot{\varphi}_p = M_p$$

Equilibrium equations (3) of the launcher-missile system:

$$k_{w11}(Y_{wst} + l_{w1}\vartheta_{wst}) + k_{w12}(Y_{wst} - l_{w2}\vartheta_{wst}) + (m_w + m_v + m_p)g = 0$$

$$\begin{aligned}
& k_{w11}l_{w1}(Y_{wst} + l_{w1}\vartheta_{wst}) - k_{w12}l_{w2}(Y_{wst} - l_{w2}\vartheta_{wst}) \\
& - k_{w31}(\vartheta_{vst} + \vartheta_{wst}) - (m_v + m_p)gh_v \sin\vartheta_{wst} = 0
\end{aligned}$$

$$k_{w31}(\vartheta_{vst} + \vartheta_{wst}) = 0$$

Figure 11 presents the parameters in the motion equations of the system, allowing for understanding of the derived dependencies. Due to the limited volume of the article, a detailed description of the physical quantities used was omitted.

Model 3

To determine the kinematic quantities characterizing the motion of the launcher after firing the missile, physical and mathematical model 3 with three degrees of freedom was formulated, Fig. 13, equations 4 and 5. As soon as the missile leaves the launcher, the gases from the rocket engine act on the launcher, Fig. 12. Only after the missile distanced from the launcher did the gases from the rocket engine cease to affect the launcher.



Fig. 12. Actual missile-launcher system

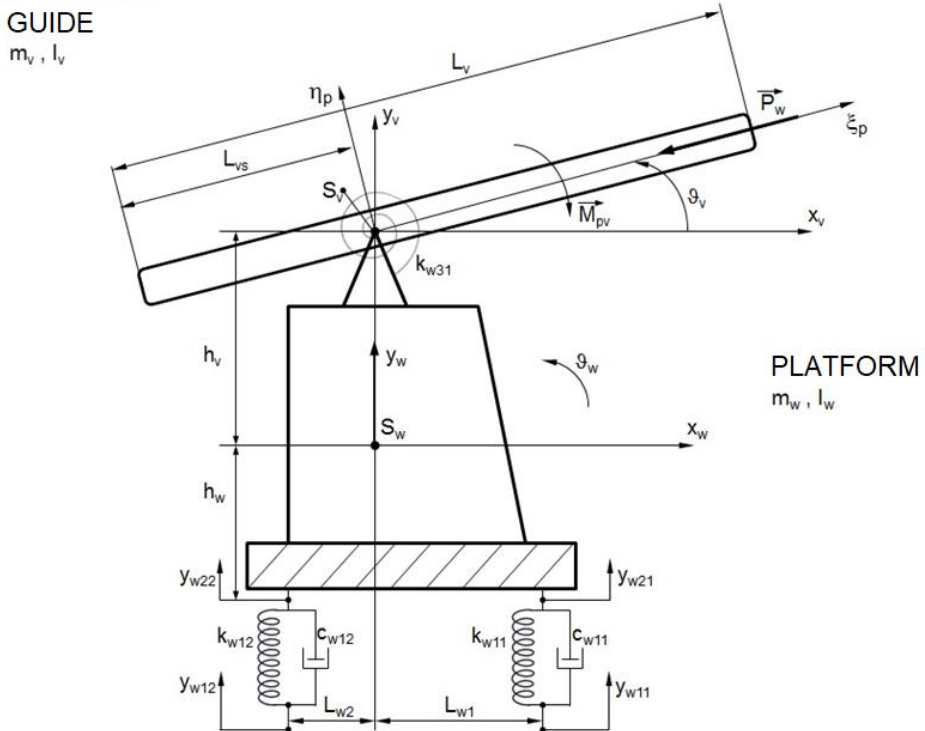


Fig. 13. Physical model of the launcher 3

Launcher motion equations (4):

Platform

$$\begin{aligned} & (m_w + m_v)\ddot{Y}_w - m_v h_v \ddot{\vartheta}_w \sin \vartheta_w - m_v h_v \dot{\vartheta}_w^2 \cos \vartheta_w \\ & + c_{w11}(\dot{Y}_w + l_{w1}\dot{\vartheta}_w - \dot{Y}_{w11}) + c_{w12}(\dot{Y}_w - l_{w2}\dot{\vartheta}_w - \dot{Y}_{w12}) \\ & \quad + k_{w11}[Y_w + Y_{wst} + l_{w1}(\vartheta_w + \vartheta_{wst}) - Y_{w11}] \\ & + k_{w12}[Y_w + Y_{wst} - l_{w2}(\vartheta_w + \vartheta_{wst}) - Y_{w12}] = -(m_w + m_v)g \\ & \quad - P_w \sin(\vartheta_v + \vartheta_w) \end{aligned}$$

$$\begin{aligned} & (I_w + I_v + m_v h_v^2)\ddot{\vartheta}_w - m_v h_v \dot{Y}_w \sin \vartheta_w + I_v \ddot{\vartheta}_v \\ & \quad + c_{w11} l_{w1}(\dot{Y}_w + l_{w1}\dot{\vartheta}_w - \dot{Y}_{w11}) \\ & - c_{w12} l_{w2}(\dot{Y}_w - l_{w2}\dot{\vartheta}_w - \dot{Y}_{w12}) - c_{w31}(\dot{\vartheta}_v - \dot{\vartheta}_w) \\ & \quad + k_{w11} l_{w1}[Y_w + Y_{wst} + l_{w1}(\vartheta_w + \vartheta_{wst}) - Y_{w11}] \\ & \quad - k_{w12} l_{w2}[Y_w + Y_{wst} - l_{w2}(\vartheta_w + \vartheta_{wst}) - Y_{w12}] \\ & - k_{w31}(\vartheta_v + \vartheta_{vst} - \vartheta_w + \vartheta_{wst}) = m_v g h_v \sin(\vartheta_w + \vartheta_{wst}) \\ & \quad + P_w h_v \cos(\vartheta_v + \vartheta_w) \end{aligned}$$

Guide

$$I_v \ddot{\vartheta}_v + I_v \ddot{\vartheta}_w + c_{w31}(\dot{\vartheta}_v - \dot{\vartheta}_w) + k_{w31}(\vartheta_v + \vartheta_{wst} - \vartheta_w + \vartheta_{wst}) = 0$$

Launcher equilibrium equations (5):

$$\begin{aligned} & k_{w11}(Y_{wst} + l_{w1}\vartheta_{wst}) + k_{w12}(Y_{wst} - l_{w2}\vartheta_{wst}) + (m_w + m_v)g = 0 \\ & \quad k_{w11} l_{w1}(Y_{wst} + l_{w1}\vartheta_{wst}) - k_{w12} l_{w2}(Y_{wst} - l_{w2}\vartheta_{wst}) \\ & \quad - k_{w31}(\vartheta_{vst} + \vartheta_{wst}) - m_v g h_v \sin \vartheta_{wst} = 0 \\ & \quad k_{w31}(\vartheta_{vst} + \vartheta_{wst}) = 0 \end{aligned}$$

Figure 13 presents the parameters in the motion equations of the system and allowing for the understanding of the derived dependencies. Due to the limited volume of the article, a detailed description of the physical quantities used was omitted.

Analysis of the launcher motion

Figure 14 shows the variability curve of the launcher's tilt angle as a function of time, recorded during experimental tests and obtained after numerical simulation of the motion of the developed theoretical model.

Considering the obtained curves, it was found that the missile-launcher system moving in the virtual space behaves in a similar way to the real assembly. The impact was thus assessed of changing the system parameters on improving the efficiency of the assembly. Figure 15 shows the variability curve of the launcher's tilt angle, obtained after numerical simulation of the motion of the developed theoretical model for the initial parameters of the system and favourably changed ones.

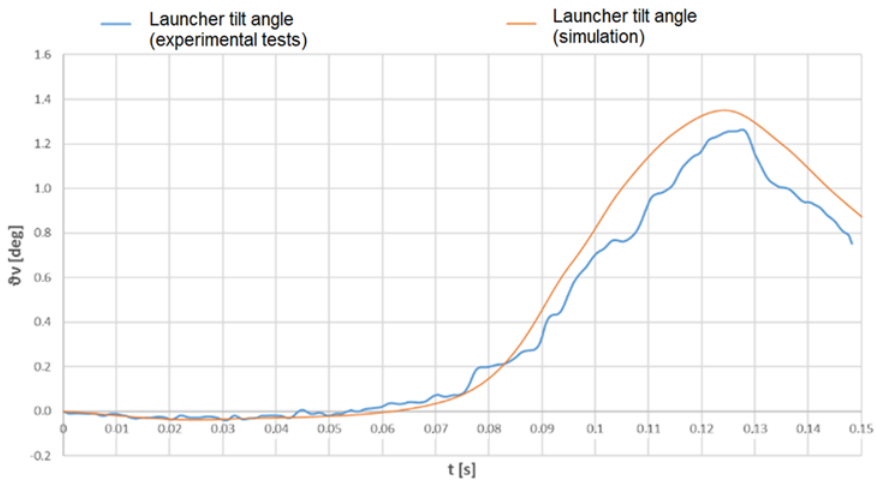


Fig. 14. Variability curve of the guide tilt angle as a function of the time obtained from the tests and the numerical simulation

If the extreme value of the guide tilt angle was reduced and its vibrations were dampened faster, the probability of hitting the target would increase. This would also reduce the time required for the effective launch of the next missile.

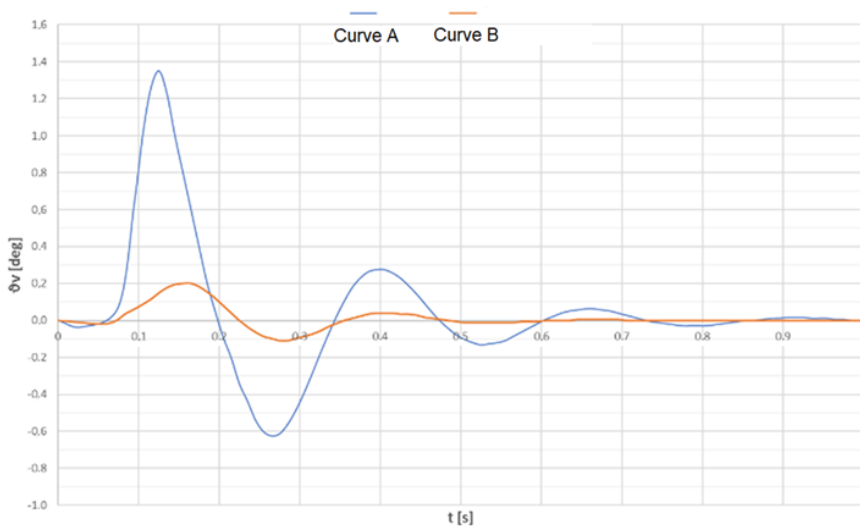


Fig. 15. Variability curve of the guide tilt angle as a function of the time obtained from numerical simulation for the initial parameters curve A and favourably changed curve B

Here we were talking about parameters that changed favourably from their initial values. The initial parameters were a set of launcher parameters for which the numerical simulation of the motion of the developed theoretical model slightly differed from the motion of the real system.

The values of the initial parameters of the launcher that affected the motion of the platform, and the guide were:

$m_w = 253$ [kg] – platform mass

$I_w = 218$ [kgm²] – platform moment of inertia

$k_{w11} = 15000$ [N/m] – front support stiffness coefficient

$c_{w11} = 2200$ [Ns/m] – front support damping coefficient

$k_{w12} = 120000$ [N/m] – rear support stiffness coefficient

$c_{w12} = 2200$ [Ns/m] – rear support damping coefficient

$L_{w1} = 1.15$ [m] – position of the front support in relation to the centre of the platform mass

$L_{w2} = 0.60$ [m] – position of the rear support in relation to the centre of the platform mass

$m_v = 84$ [kg] – guide mass

$I_v = 73$ [kgm²] – guide moment of inertia

$k_{w31} = 200000$ [N/m] – stiffness coefficient of the guide mounting on the platform

$c_{w31} = 5000$ [Ns/m] – damping coefficient of the guide mounting on the platform

Favourably changed values of system parameters that had a significant impact on the motion of the platform and the guide were:

$m_w = 278$ [kg] – platform mass

$I_w = 240$ [kgm²] – platform moment of inertia

$k_{w11} = 120000$ [N/m] – front support stiffness coefficient

$c_{w11} = 3500$ [Ns/m] – front support damping coefficient

$k_{w12} = 120000$ [N/m] – rear support stiffness coefficient

$c_{w12} = 3500$ [Ns/m] – rear support damping coefficient

$L_{w1} = 1.00$ [m] – position of the front support in relation to the centre of the platform mass

$L_{w2} = 0.75$ [m] – position of the rear support in relation to the centre of the platform mass

$m_v = 94$ [kg] – guide mass

$I_v = 80$ [kgm²] – guide moment of inertia

$k_{w31} = 220000$ [N/m] – stiffness coefficient of the guide mounting on the platform

$c_{w31} = 5500$ [Ns/m] – damping coefficient of the guide mounting on the platform

4. CONCLUSIONS

The study and analysis of the dynamic phenomena occurring in the self-propelled anti-aircraft assembly is a complex task that requires the consideration of many interactions [8]. The study attempts to analyse the interaction of the assembly objects on the example of the ZSMU-70 weapon module.

The results allowed for the development of several guidelines aimed at shaping the dynamic characteristics of the WW-4 launcher to increase the effectiveness of the assembly. Due to the introduction of parameters favourably changing the dynamics of the launcher, the extreme value of the tilt angle of the guide decreased and, at the same time, its vibrations were damped much quicker, which resulted in an increased probability of hitting the target. As a result, the time after which the probability of hitting the target with the next missile also decreased. Empirical and theoretical analysis identified changes in the design and parameters of the system, including:

- Increasing the mass and moment of inertia of the platform.
- Increasing the stiffness and damping coefficient of the front and rear supports. In particular, increasing the stiffness of the front support to the stiffness value of the rear support.
- Decreasing the position of the front support in relation to the mass centre of the platform and increasing the position of the rear support in relation to the mass centre of the platform.
- Increasing the mass and moment of inertia of the guide.
- Increasing the stiffness and damping coefficient of the guide mounting on the platform.

FUNDING

The authors received no financial support for the research, authorship, and/or publication of this article.

REFERENCES

- [1] Genta, Giancarlo. 1997. *Motor Vehicle Dynamics, Modeling and Simulation*. Singapore: World Scientific Publishing.
- [2] Gillespie, D. Thomas. 1992. *Fundamentals of Vehicle Dynamics*. SAE International.
- [3] Swetlicky, A. Walery. 1963. *Launch dynamics of flying objects* (in Russian). Moscow: Science.
- [4] Dziopa, Zbigniew, Zbigniew Koruba, and Izabela Krzysztofik. 2010. "An analysis of the dynamics of a launcher–missile system on a moveable base". *Bulletin of the Polish Academy of Sciences – Technical Sciences* 58 (4) : 645-650.
- [5] De Silva, W. Clarence. 2007. *Vibration Fundamentals and Practice*. London – New York: Taylor & Francis Group.
- [6] Gantmacher, Felix Ruvimovich. 1970, *Lectures in analytical mechanics*, (translated from Russian by G Yankovsky). Moscow: Mir publishers.

- [7] Dziopa Zbigniew, and Maciej Nyckowski. 2015. „Wpływ dyssypacji energii w układzie wyrzutnia-samochód na warunki startu rakiety niesterowanej”. *Problemy mechatroniki. Uzbrojenie, lotnictwo, inżynieria bezpieczeństwa* 6 (4): 55-68.
- [8] Dziopa Zbigniew. 2008. *Modelowanie i badanie dynamicznych właściwości samobieżnych przeciwlotniczych zestawów raketowych*. Monografie, Studia, Rozprawy M9. Kielce: Politechnika Świętokrzyska.

Modelowanie i badanie dynamicznych właściwości wyrzutni z niesterowanymi pociskami raketowymi

Zbigniew J. DZIOPA¹, Maciej NYCKOWSKI²

¹Politechnika Świętokrzyska,

Al. Tysiąclecia Państwa Polskiego 7, Kielce

²Sieć Badawcza Łukasiewicz – Instytut Lotnictwa,

Al. Krakowska 110/114, Warszawa

Streszczenie. W pracy przeprowadzono analizę działania modułu uzbrojenia ZSMU-70. Otrzymane wyniki pozwoliły na opracowanie kilku wytycznych, zmierzając do takiego kształtowania właściwości dynamicznych wyrzutni WW-4, aby poprawić skuteczność modułu ZSMU-70. W związku z tym zrealizowano badania eksperymentalne na poligonie wojskowym. Wykonano strzelania niesterowanymi pociskami raketowymi NLPR-70. Proces strzelania zarejestrowano za pomocą szybkiej kamery cyfrowej Phantom. Następnie poddano analizie zarejestrowane obrazy za pomocą oprogramowania TEMA. Na podstawie wyników badań empirycznych sformułowano model fizyczny i matematyczny ruchu zarówno modułu ZSMU-70, jak i wyrzutni WW-4. Opracowano program komputerowy i przeprowadzono symulację ruchu układu podczas wystrzeliwania pocisków raketowych. Uzyskane z analizy teoretycznej wyniki porównano z analogicznymi wynikami otrzymanymi z badań empirycznych. Mając zweryfikowany model teoretyczny, zmieniono niektóre parametry układu i uzyskano wytyczne umożliwiające poprawę skuteczności modułu uzbrojenia ZSMU-70.

Słowa kluczowe: inżynieria mechaniczna, wyrzutnia, pociski raketowe, badania empiryczne, analiza teoretyczna



This article is an open access article distributed under terms and conditions of the Creative Commons Attribution-NonCommercial-NoDerivatives International 4.0 (CC BY-NC-ND 4.0) license (<https://creativecommons.org/licenses/by-nc-nd/4.0/>)